Title:	Punching shear strength of R/C slabs subjected to fire
Authors:	Bamonte P., Fernández Ruiz M., Muttoni A.
Published in:	Proceedings of the 7th International Conference on Structures in Fire - SiF2012 (Eds. M. Fontana, A. Frangi, M. Knobloch)
Pages:	pp. 689-698
Year of publication:	2012
Type of publication:	Peer reviewed conference paper

Please quote as:	Bamonte P., Fernández Ruiz M., Muttoni A., *Punching shear strength of R/C slabs subjected to fire*, Proceedings of the 7th International Conference on Structures in Fire - SiF2012 (Eds. M. Fontana, A. Frangi, M. Knobloch), 2012, pp. 689-698.

7th International Conference on Structures in Fire
M. Fontana, A. Frangi, M. Knobloch (Eds.)
Zurich, Switzerland, June 6-8, 2012

PUNCHING SHEAR STRENGTH OF R/C SLABS SUBJECTED TO FIRE

Patrick Bamonte*, Miguel Fernández Ruiz and Aurelio Muttoni****

* Politecnico di Milano, Milan, Italy
e-mail: patrick.bamonte@polimi.it

** École Polytechnique Fédérale de Lausanne, Lausanne, Switzerland
e-mails: miguel.fernandezruiz@epfl.ch, aurelio.muttoni@epfl.ch

Keywords: punching shear, flat slabs, Critical Shear Crack Theory.

Abstract. *This paper illustrates a study on the punching shear strength of reinforced concrete slabs in fire conditions. To this end, a set of experimental data on the punching strength of heated slab specimens was interpreted by adapting the well-known Critical Shear Crack Theory to include the effects of high temperature and fire. The comparison between experimental and numerical results is rather good, considering the several uncertainties affecting the problem under consideration. It turns out that the proposed approach is a reliable tool to evaluate the punching strength of thermally-damaged slabs, and this is a good premise for a more in-depth study of the behaviour of punching-sensitive flat slabs in fire conditions.*

1 INTRODUCTION

Fire has traditionally represented a real threat to the safety of buildings and civil structures. As it is well known, the effects of high temperature on structures are two-fold: (a) the mechanical properties of the building materials, such as strength and stiffness to name the most important, are adversely affected by temperature; and (b) the thermal dilation and the ensuing deformations and displacements bring in supplementary "indirect actions", that can, generally speaking, significantly increase the internal forces with respect to the values in ordinary conditions. The synergy of these two effects can be particularly detrimental, whenever a significant decay of the strength, and therefore of the bearing capacity of structural members, is accompanied by an increase of the state of stress.

A typical way of tackling this problem, from the point of view of structural safety, is to compare the bearing capacity at a given section of a structural member, with the internal force at the location, both functions of the fire duration. The calculation of the bearing capacity as a function of the fire duration is usually carried out by making reference to the classic assumptions of structural mechanics (for example, in the case of beams and columns). The effects of high temperature are then taken into account by reducing the strength and stiffness of the materials at each point of the given section, on the basis of the temperature ensuing from the fire exposure. Several works in the related literature illustrate this kind of approach for common structural members [1,2], and simplified and designer-friendly methods are available in the codes [3]. The evolution of the internal forces with the fire duration, on the contrary, is a highly non-linear problem, that requires the use of sophisticated numerical techniques, and is therefore rather demanding from the computational point of view [4,5]. A possible alternative to overcome these problems is to resort to classic limit analysis, that makes it possible to avoid structural analysis, and therefore greatly simplifies the safety verifications in the time domain. Such an approach is particularly advantageous in highly-redundant and complex structures, where performing a fully non-linear structural analysis is rather demanding, and, from the designer's point of view, almost prohibitive.

The possibility of using a plastic approach in fire is limited, as in ordinary conditions, by premature brittle failures, like, for instance, shear in beams and columns, and punching shear in slabs. The former is

certainly a big problem in columns of frame structures, where the thermal dilation of beams induces an additional shear force in the columns. It is fair to say, however, that shear failures in fire are rather uncommon [3]. In the case where they are of concern, the main driving parameter is, as it is usually the case in compact under-reinforced sections, the transverse reinforcement [6], and not the concrete, unless, for example, in the case of precast members with rather thin sections [7].

As for punching shear in slabs, the problem is of much more significance, because more or less significant increases of the internal forces (and, therefore, of the punching forces) are to be expected in the case of fire [8] (Fig. 1).

Moreover, a significant role in the punching resistance is played by concrete tensile strength and aggregate interlock; these two effects are both taken into account in some way in the current design equations of the most popular standards [9]. It is fair to say, however, that the aforementioned code equations were obtained on a semi-empirical basis, by operating a regression of the available experimental data: an immediate extension of these expressions to the case of fire is, therefore, highly questionable, to say the least. To tackle the problem of the punching shear resistance in fire in a rational way is only then possible, if reference is made to a physical-based model, such as the "critical shear crack" theory, that was developed during the last years at the EPFL in Lausanne, in the framework of a vast experimental campaign, with some 100 slab specimens tested in punching [10,11].

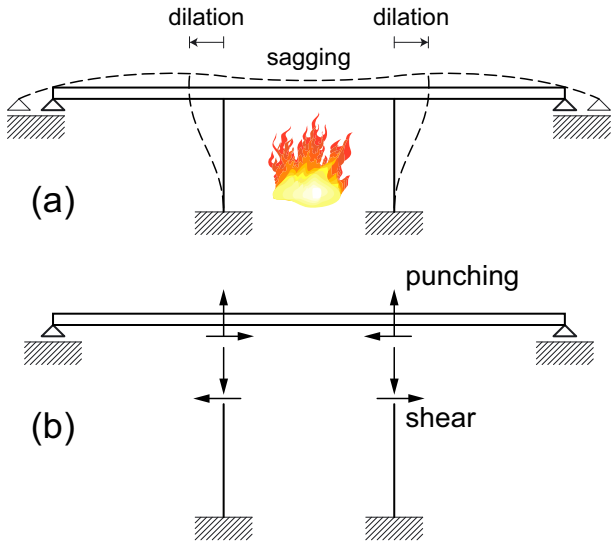

Figure 1. Flat slabs in fire: (a) temperature-induced displacements; and (b) indirect actions.

Despite the wide-spread use of reinforced concrete slabs, no adequate attention has been devoted so far to punching shear in fire. Nevertheless, the topic is of interest, because of the large use of slabs in fire-sensitive structures (like, for example, underground garages), and also in buildings.

In this paper, an extension of the critical shear crack theory to the case of fire is presented. The main assumptions of the model are adapted to incorporate the effects of high temperature, i.e. the two backbone curves of the model (namely, the failure criterion and the load-deformation curve) are modified in order to account for the thermal-induced strength decay and deformability increase. The extension of the model is validated against the few available experimental data, and some design-oriented conclusions are drawn.

2 EXPERIMENTAL DATA

Punching shear of slabs in ambient conditions has been extensively investigated in the past (both experimentally and theoretically). In the case of slabs in fire, however, no adequate attention has been devoted so far to punching shear, and only two references can be cited: the first about the residual behaviour of small circular slabs [12], where a few design equations commonly used at ambient temperature are extended to cover the case of high temperature exposure, and the second on real-scale fire tests on two-way slabs [13]. In the following, reference will be made to the latter; to this end, in this section the main features of the tests are briefly recalled.

Ten specimens were cast and tested; the choice of the specimens' dimensions, as well as of the test set-up, were calibrated on the basis of (a) the prescriptions of the Eurocode 2 (1992 version); and (b) previous tests in fire conditions carried out at the Technical University of Braunschweig (Germany).

The test set-up is shown in Figs. 2a and b. The specimens consist of square slabs (dimensions = 250 × 250 × 20 cm^3) with a short column "stub" (dimensions = 25 × 25 × 40 cm^3) in the middle.

At the top of the loading frame, the specimens are loaded through a hollow-core hydraulic jack. On the bottom the load is applied through a tendon (∅ = 36 mm, St 1080/1230), provided with thermal insulation, that passes through a hole in the specimen, and is anchored to the bottom face of the column stub at one end, and to the hydraulic jack at the other. The proper distribution of the load from the tendon to the column is achieved through a 50 mm-thick steel plate. The column stub is insulated during the whole fire duration, by means of vermiculite plates (thickness = 100 mm). On the top of the slabs, the load is transferred from the tendon to two HEM 260 beams, that are supported by the loading frame, namely a 400 mm-thick plate with an octagonal hole in the centre portion. The load is then transferred from the frame to the specimen by means of 16 loading points, that are uniformly distributed over a circle (diameter ∅ = 220 cm). The applied load is measured through a load cell, that is placed at the top end of the tendon. The overall dimensions of the furnace chamber are 230 × 230 ×100 cm^3. The whole test set-up (specimen + loading frame + loading devices) is supported by reaction bearings, that are positioned on the perimeter of the furnace area (side = 230 cm), at a distance of approximately 75 cm from each other.

It is worth noting that the punching load applied to the specimen results from a self-equilibrated system; in other words, the punching action is a sort of prestressing load applied via the tendon at the bottom, and through the 16 loading points on top: therefore, the state of stress and deformation resulting from the punching load is approximately axisymmetric. As for the heating, a standard temperature-time curve (ISO-834) was adopted in all cases.

Following are the main characteristics of the tested specimens:

- thickness = 200 mm, axis distance to the reinforcement (= gross cover) ≈ 35 mm;
- effective depth = 167 mm;
- geometric reinforcement ratio over the column stub: two values (0.50 and 1.50%) were adopted;
- three specimens were provided with "hat-type" shear reinforcement.

Figs. 3a,b shows the layout of the reinforcement in one quarter of specimen, for the two groups of specimens (with light and heavy reinforcement, respectively). The properties of the materials used in the specimens are as follows:

- concrete compressive strength: f_c^{20} = 35-52 MPa
- yield strength of bending reinforcement: f_y^{20} = 504-590 MPa
- yield strength of transverse reinforcement: f_y^{20} = 533 MPa

Finally, it is worth mentioning that 5 out of 10 tested slabs underwent spalling on the heated face. The spalling depth was in most cases approximately equal to the gross cover (≈ 40 mm); in one case (Slab 9) spalling was limited to 20 mm.

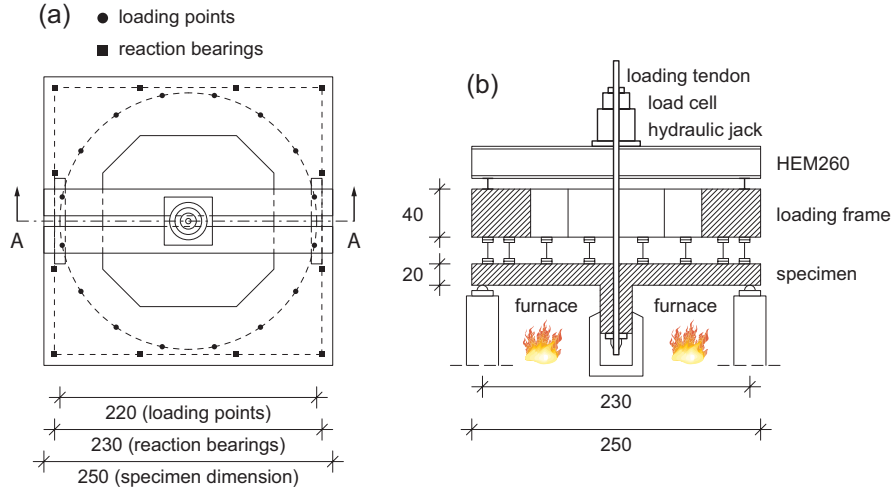

Figure 2. Test set-up (adapted from [13]): (a) top view; and (b) section cut along A-A.

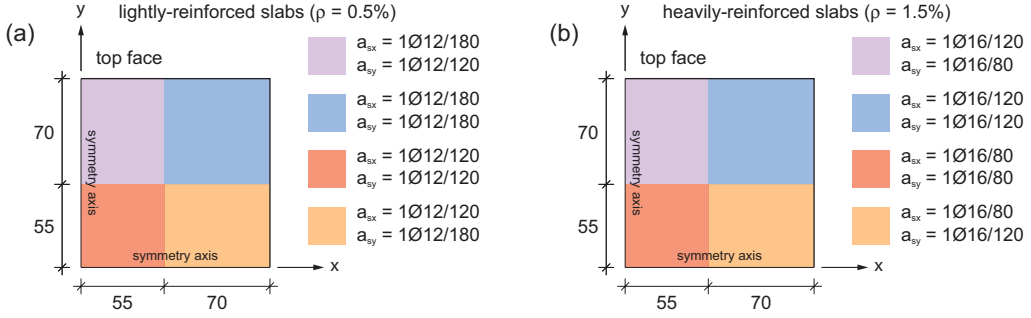

Figure 3. Layout of the negative reinforcement: (a) lightly-reinforced slabs (ρ = 0.5%); and (b) heavily-reinforced slabs (ρ = 1.5%).

The load at the beginning of each test was calibrated on the basis of the design load in fire conditions as per Eurocode = 0.7 × punching resistance at room temperature. In most cases (8 slabs out of 10), the load was increased during the first 30 minutes by variable amounts (0%-70%), to simulate the load redistribution that could potentially take place in an actual flat slab exposed to fire. Beyond 30 minutes, the load was kept constant throughout the whole duration of the test. In the cases, where the specimens stood the constant load phase without collapsing, they were loaded to failure at the end of the heating process. The failure loads and times to failure of the 10 specimens are summarized in Table 1.

Table 1. Summary of the failure loads and times to failure of the specimens tested by Kordina [10].

specimen	1	2	3	4	5	6	7	8	9	10
test duration [min]	120	120	27	17	90	90	29	70	90	22
failure load [kN]	492	475	550	810	386	380	500	568	410	460

3 THEORETICAL MODEL

The model developed to interpret the behaviour of the slabs described in the previous section is an extension of the Critical Shear Crack Theory (CSCT) [10,11] to the case of high temperature and/or fire. This theory, that has been demonstrated to provide a reliable tool for estimating the punching resistance of flat slabs in ordinary conditions, is first briefly recalled; following, the modifications introduced to take the effects of high temperature into account are outlined.

3.1 CSCT – Original formulation

The Critical Shear Crack Theory is a semi-empirical approach, aimed at the evaluation of the punching resistance of flat slabs. It was originally developed for axisymmetric slabs without shear reinforcement, and later on adapted to take into account the role played by the various types of shear reinforcement. The main assumption is that in a slab-column assembly subjected to the highly-concentrated load of a column, a diagonal shear crack will form, where the deformations will localize. As a consequence, in an axisymmetric layout, the deflected shape outside the crack will be conical, i.e. the downward displacement will be linear, and the rotation Ψ constant. This assumption greatly simplifies the description of the structural behaviour, that can be expressed as a closed-form load-rotation relationship of the slab-column assembly.

The increase of the rotation Ψ upon increasing external applied loads is limited by the ability of the critical diagonal shear crack to transfer the shear stresses: the explanation is that the crack opening increases with increasing rotation Ψ, and thus the aggregate interlock, that is responsible for carrying most of the shear stresses, is reduced. On the basis of several experimental data from different authors, a semi-empirical failure criterion was worked out, to relate the rotation of the slab portion surrounding the column, and the shear force that can be transmitted across the diagonal crack (Fig. 4a):

$$\frac{V_u}{b_0 \cdot d \cdot \sqrt{f_c}} = \frac{3/4}{1+15 \cdot \frac{\Psi d}{d_{g0}+d_g}} \tag{1}$$

where b_0 is the critical perimeter, d is the effective depth of the reinforcing bars close to the extrados, f_c is the compressive strength of concrete, d_g is the maximum aggregate size, and d_{g0} is a reference aggregate size. Note that whereas the second member of Eq. (1) takes into account the detrimental effect of increasing crack width on aggregate interlock, the denominator of the first member accounts for the strength of the highly-stressed concrete in compression close to the face of the column.

The punching failure occurs when the load-induced rotation is such, that the shear force can no longer be transferred through the crack. From the analytical point of view, the punching failure is determined by the intersection between the load-rotation curve (that represents the structural response of the slab-column assembly), and the failure criterion (Fig. 4b), expressed by Eq. (1).

3.2 Extension of CSCT to high temperature

Being largely based on a clear framework of reasonable mechanical assumptions, the CSCT can be efficiently adapted to cover the case of flat slabs subjected to high temperature.

The main assumption of the theory, namely that a diagonal shear crack forms at early loading stages and influences the behaviour of the whole slab-column assembly, is retained as such.

As for the displacement profile along the slab, a preliminary distinction should be introduced:

$$w_{tot} = w_{load} + w_{th} \tag{2}$$

where w_{tot} is the total displacement, w_{load} is the load-induced (or mechanical) displacement, and w_{th} is the thermal displacement.

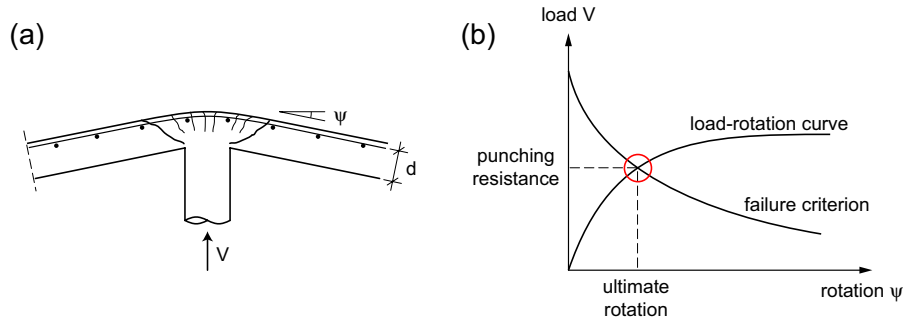

Figure 4. Critical Shear Crack Theory: (a) typical slab-column assembly considered; and (b) determination of the punching resistance in the load-rotation domain.

The load-induced displacement w_{load} is the displacement that ensues from the applied load: it is affected by high temperature, because of the temperature-induced materials' decay, that brings in a stiffness decay (in regions subjected to negative bending mainly because of the reduction of the effective depth), and, upon prolonged fire durations, also the decay of the ultimate strength.

The thermal displacement w_{th} is the deflection caused by thermal sagging, that in turn originates from the thermal dilation of the hot layers of material, and the ensuing thermal curvature on the slab's thickness. The following assumptions are introduced:

a) outside the diagonal crack, the load-induced rotation Ψ is constant: therefore, the load-induced displacement w_{load} is a linear function of the radial coordinate, outside the diagonal crack (Fig. 5a);
b) the thermal displacement w_{th} is a 2^{nd}-order parabola of the radial coordinate (Fig. 5b).

The first assumption implies that, upon loading, the kinematic behaviour of the slab sector is similar to that in ordinary conditions, the only difference being the aforementioned stiffness reduction ensuing from the thermal damage.

The second assumption originates from the consideration that in an axisymmetric slab sector subjected to uniform heating, the radial and tangential thermal curvatures are also uniform: therefore, the deflected shape ensuing from the thermal curvatures is spherical, or, with the usual first-order approximation on the radius of curvature, a 2^{nd}-order parabola. It is worth noting that if the edge of the slab is simply supported, a spherical deflected shape implies neither radial nor tangential bending moments, i.e. a uniform distribution of thermal curvatures is not restrained by the boundaries.

A key point in the previous assumptions is the concept of "thermal curvatures": as a matter of fact, in a slab subjected to high temperature and high heating rates, the thermal gradient along the thickness is non-linear. Moreover, when concrete is heated well above ambient temperature, the dilation coefficient is highly temperature-dependent, at least below 700°C. As a consequence, the free thermal strains along the thickness are not linear, and therefore a free thermal curvature as such (i.e. the slope of a linear distribution of free thermal strains) cannot be defined. Fig. 6 shows the typical moment-curvature diagrams in pure bending of a slab section subjected to heating from below. It is worth noting that the decay of stiffness and ultimate capacity is more pronounced in positive bending, as should be expected, since the bottom reinforcement undergoes a significant temperature increase. Most notably, however, there is a translation of the diagrams towards the positive curvatures, that increases with increasing fire duration: in other words, the section will undergo a thermal curvature, even if no load is applied on the section (M = 0). In the following, on the basis of the previously-introduced decomposition of the displacements, the thermal curvature is defined as the intersection between the diagrams and the horizontal axis, i.e. the curvature corresponding to no bending moment applied. The diagrams deprived of the contribution of the thermal curvature are "moment vs. load-induced curvature" diagrams, and can be used to work out the load-induced displacement w_{load} (Fig. 5a).

Note that, if the thermal curvature and the relationship between moment and load-induced curvature are defined by means of the aforementioned approach, the superposition principle can be applied, because the different non-linear phenomena taking place on the section (i.e. the self-stresses ensuing from the non-linear thermal strains) are implicitly taken into account in the calculation of the moment curvature diagram.

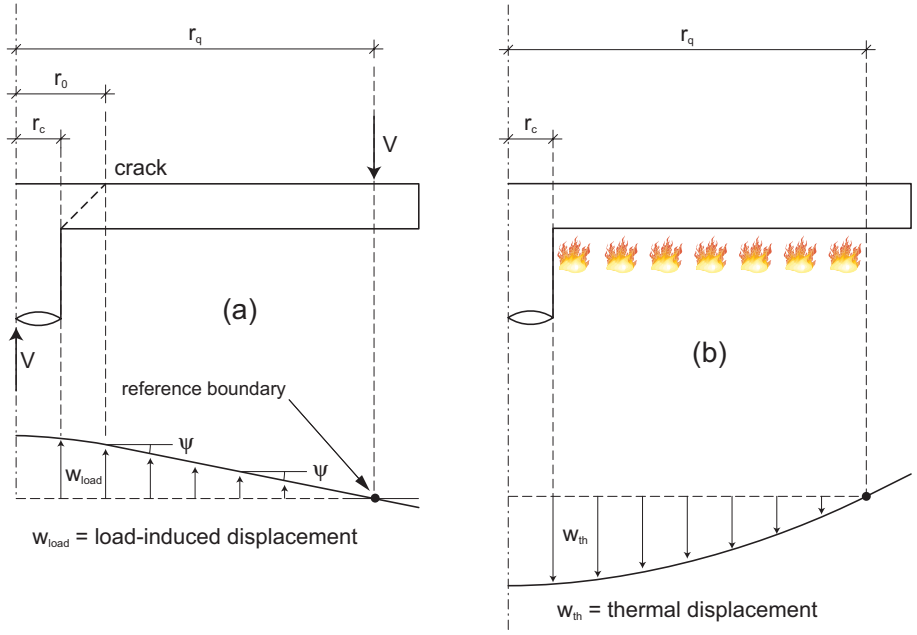

Figure 5. Displacement decomposition at high temperature: (a) load-induced displacement; and (b) thermal displacement.

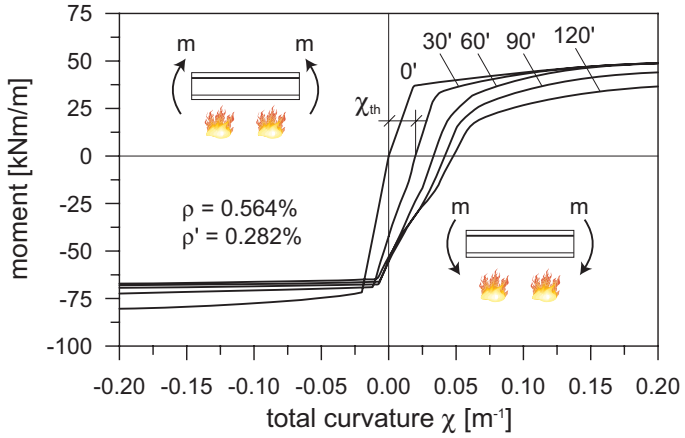

Figure 6. Typical moment-curvature diagrams of the lightly-reinforced slabs tested in [10].

As for the failure criterion, the effects of fire have to be taken into account separately. Considering Eq. (1), the square root of the compressive strength is related to the post-peak softening branch in

compression, or to the toughness in tension. An in-depth investigation of these aspects, however, is beyond the scope of this paper; moreover, it would require a significant number of experimental data on shear failures of plain concrete members at high temperature. Therefore, the decay of this term is evaluated by simply considering an average reduction of the compressive strength along the thickness, or, equivalently, by reducing the effective depth on the basis of the decay of the compressive strength. As the critical perimeter is proportional to the effective depth, also b_0 undergoes a similar reduction.

The denominator of the second member of Eq. (1), that takes into account the decrease of aggregate interlock with increasing crack opening, should be reduced in a similar way, since the reduction of the effective depth will increase the crack opening. This fact, however, is implicitly taken into account by the fact that the rotation used in the failure criterion is the load-induced rotation, and therefore it increases with the reduction of the bending stiffness (as evaluated in the moment-curvature diagrams). It could be argued, however, that the rotation to be considered in the failure criterion is the total rotation, which is smaller because of the contribution of the thermal rotation. There are two main reasons to make reference to the sole load-induced rotation (i.e. to neglect the thermal rotation): (a) in the vicinity of the column, the rotations ensuing from the thermal displacements are small; (b) compared to the load-induced rotation, the thermal rotation is favourable, because its effects are opposite to those ensuing from the load applied.

4 COMPARISON BETWEEN EXPERIMENTAL AND NUMERICAL RESULTS

The proposed extension of the CSCT was validated by simulating the experimental results. The comparisons were carried out both in terms of load-total displacement curves, as well as with reference to the ultimate load.

The first task is accomplished by working out, for any given fire duration, the relation between the load and the mechanical rotation. By considering, for the same fire duration, the applied load (as per load protocol used in the tests) the mechanical rotation can be worked out by means of the moment-curvature diagrams, and the displacement at the face of the column is then calculated by applying the previous kinematic assumption concerning the load-induced displacement. As for the thermal displacement, it can be worked out directly, by integrating the thermal curvature for any given fire duration. The failure load is evaluated by means of the procedure illustrated in Fig. 4b, i.e. as the intersection between the load-rotation curve and the failure criterion for the maximum fire duration reached during the test.

The decay of the mechanical properties and the thermal dilation, in lack of more accurate information, were evaluated according to the provisions of Eurocode 2 [3], assuming the properties of a calcareous concrete. As for the thermal properties, the value of the thermal conductivity was back-fitted, in order to have thermal profiles in good agreement with those provided in [13].

Fig. 7 shows the comparison between the experimental and numerical results, expressed in terms of net deflection (= total deflection devoid of the deflection at the onset of heating) at the centre of the slab, as a function of the fire duration. It is worth noting that the net deflection is always positive (= downward), even though the load at the centre of the slab is directed upward: this indicates that in the tests under consideration the role of the thermal curvature prevails over the load. Most notably is also that in Fig. 7a, Slab 2 exhibits a smaller net displacement than Slab 1 as should be expected, since the load applied to the former (and maintained constant throughout the whole test) was higher than the load applied to the latter.

Fig. 8 illustrates the application of the proposed approach for the evaluation of the failure load; in both cases, the load-rotation curve and the failure criterion were evaluated taking into account the thermal damage corresponding to the time of failure. On the whole, the agreement between the numerical and the experimental failure load (represented by the horizontal dashed line) is satisfying. Moreover, it is interesting to observe that the failure in lightly-reinforced slabs (Fig. 8a) occurs when the load-rotation curve is very close (or even at) the yield plateau, i.e. in lightly-reinforced slabs, even in the case of exposure to fire, the ultimate punching load corresponds to a ductile failure. On the contrary, the heavily-

reinforced slab considered (Fig. 8b) reaches its ultimate load in the ascending phase of the load-rotation curve, i.e. the punching failure occurs prior to yielding of the reinforcement.

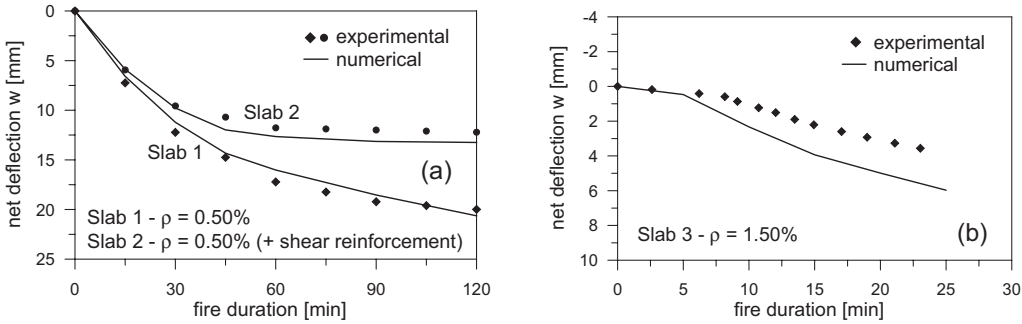

Figure 7. Comparison between experimental and numerical displacement at the centre of the slabs as a function of the fire duration: (a) lightly-reinforced slabs (ρ = 0.50%); and (b) heavily-reinforced slab (ρ = 1.50%).

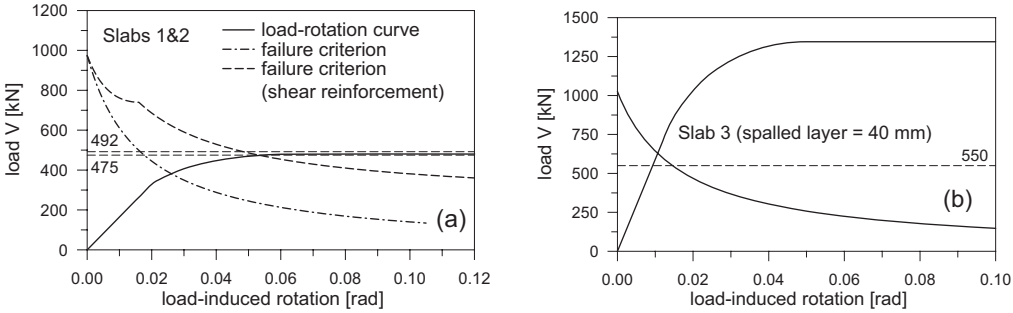

Figure 8. Evaluation of the failure load: (a) lightly-reinforced slabs (ρ = 0.50%); and (b) heavily-reinforced slab (ρ = 1.50%).

5 CONCLUDING REMARKS

On the basis of the preliminary results presented in this paper, the following conclusions can be drawn:

- the Critical Shear Crack Theory, that is used in ordinary conditions to work out the punching resistance of flat slabs, provides a rational tool to study the punching shear strength of flat slabs in fire conditions;
- the numerical fitting of the experimental results taken into consideration is rather good, with respect to both the structural behaviour (displacement vs. fire duration) and to the failure load.

Further research is needed in order to clarify several aspects, such as (a) the role of membrane stresses, that are rather important whenever the structural layout is such that the thermal elongations are restrained (something that did not occur in the tests considered herein); and (b) the possibility of evaluating the bearing capacity in punching by simply adapting the code equations available for ordinary conditions.

REFERENCES

[1] Meda, A., Gambarova, P.G., and Bonomi, M., "High-Performance Concrete in Fire-Exposed Reinforced Concrete Sections," *ACI Structural Journal*, V. 99, No. 3, pp. 277-287, May-June 2002.

[2] Caldas, R.B., Sousa, J.B.M., Hallal Fakury, R., "Interaction diagrams for reinforced concrete sections subjected to fire", *Engineering Structures*, V. 32, No. 9, pp. 2832-2838, 2010.

[3] CEN, European Committee for Standardization. EN 1992–1–2, Eurocode 2: Design of concrete structures – Part 1–2: General rules – Structural fire design, Brussels, Belgium, 2004.

[4] Riva, P., and Franssen, J.-M., "Structural Behaviour of Continuous Beams and Frames," Chapter 4 in *fib* Bulletin 46: "Fire Design of Concrete Structures—Structural Behaviour and Assessment,", 210 pp, 2008.

[5] Biondini, F., and Nero, A., "Cellular Finite Beam Element for Nonlinear Analysis of Concrete Structures under Fire", *ASCE Journal of Structural Engineering*, V. 137, No. 5, pp. 543-558, 2011.

[6] Faria, R., Xavier, H.F., and Vila Real, P. "Simplified Procedure for Shear Failure Assessment of RC Framed Structures Exposed to Fire", *Structures in Fire – Proceedings of the Sixth International Conference*, V. Kodur, J.-M. Franssen (eds.), DEStech Publications, Lancaster, pp. 197-205, 2010.

[7] Bamonte, P., Felicetti, R., Gambarova, P.G., and Giuriani, E., "Thin-Walled Open-Section P/C Beams in Fire: A Case Study", *fib* Bulletin 57 "Shear and punching shear in RC and FRC elements", pp. 173-193, 2011.

[8] Bamonte, P., Felicetti, R., and Gambarova, P.G., "Punching Shear in Fire-Damaged Reinforced Concrete Slabs", *ACI Special Publication 265 "Thomas T.C. Hsu Symposium on Shear and Torsion in Concrete Structures"*, pp. 345-366, 2009.

[9] CEN, European Committee for Standardization. EN 1992–1–1, Eurocode 2: Design of concrete structures – Part 1–1: General rules and rules for buildings, Brussels, Belgium, 2004.

[10] Muttoni, A., "Punching Shear Strength of Reinforced Concrete Slabs without Transverse Reinforcement," *ACI Structural Journal*, V. 105, No. 4, pp. 440-450, July-August 2008.

[11] Fernández Ruiz, M., and Muttoni, A., "Applications of Critical Shear Crack Theory to Punching of Reinforced Concrete Slabs with Transverse Reinforcement", *ACI Structural Journal*, V. 106, No. 4, pp. 485-494, July-August 2009.

[12] Felicetti, R., and Gambarova, P. G., "On the Residual Behavior of HPC Slabs Subjected to High Temperature," *PCI/FHWA/FIB International Symposium on High-Performance Concrete*, Orlando, FL (USA), pp. 598-607, September 2000.

[13] Kordina, K., "Über das Brandverhalten punktgestützter Stahlbetonplatten" (On the Fire Behavior of Reinforced Concrete Flat Slabs), *Deutscher Ausschuss für Stahlbeton (DAfStb)*, Berlin (Germany), Heft 479, 106 pp, 1997.